

Supporting Information

Zhou et al. 10.1073/pnas.1409701111

Models and Computational Details

First-principles electronic structure calculations based on density functional theory (DFT) were carried out using the plane-wave-basis-set and the projector-augmented-wave method (1, 2), as implemented in the Vienna ab initio package code (3). The energy cutoff was set to 500 eV. For the exchange and correlation functional, the generalized gradient approximation (GGA) in Perdew–Burke–Ernzerhof (PBE) format (4) was used. The calculation was further verified by using the more sophisticated Heyd–Scuseria–Ernzerhof hybrid functional (5), which made no essential difference (Fig. S1). Spin-orbit coupling (SOC) is included by a second variational procedure on a fully self-consistent basis.

Si(111) surfaces were modeled by using a slab geometry of 10 atomic layers, with a vacuum region of 30 Å in the direction normal to the surface. Test calculations were performed by using larger thickness (12 and 16 layers), which gave similar results. The bottom Si surfaces were terminated by H atoms in a monohydride form. During structural optimization, both the 10th layer of Si atoms and the H atoms saturating them were fixed and all other atoms were fully relaxed until the atomic forces are smaller than 0.01 eV/Å. A $15 \times 15 \times 1$ Γ -centered k -point mesh was used to sample the Brillouin zone. Dipole corrections were also tested and found making little difference.

For epitaxial growth of Bi and Au atoms on the one-third X-covered Si(111) surface (X = Cl, Br, I), we considered a $\sqrt{3} \times \sqrt{3}$ supercell and different adsorption configurations. The energy barriers for Bi hopping on the Si(111) surfaces were calculated by using the climbing-image nudged elastic band method (6).

Z_2 invariant calculations were performed by using the full-potential linearized augmented plane-wave method (7) within the GGA-PBE functional including SOC. A converged ground state was obtained using 5,000 k points in the first Brillouin zone and $K_{\max} \times R_{\text{MT}} = 8.0$, where K_{\max} is the maximum size of the reciprocal lattice vectors and R_{MT} denotes the muffin-tin radius. Wave functions and potentials inside the atomic sphere are expanded in spherical harmonics up to $l = 10$ and 4, respectively. For Z_2 calculation, we follow the method by Fukui et al. (8), to directly perform the lattice computation of the Z_2 invariants from first principles.

Results by Using Hybrid Functional from Ref. 5

Band structures of Bi@Br(I)-Si(111)

We also calculated band structures of hexagonal Bi lattice grown on Si(111)- $\sqrt{3} \times \sqrt{3}$ -Br and -I surfaces without and with SOC, as shown in Fig. S2. They show similar electronic properties and SOC-induced band-gap opening as those of Bi@Cl-Si(111) (Fig. 2A and C).

It is interesting to note that the Bi-related energy bands become more dispersive for Bi@Br-Si(111) and Bi@I-Si(111) surface. This results from different interaction strength between Bi atoms mediated by different halogen ions on the surface. Going from Cl to Br and to I, the ionic radius gradually increases from 1.81 to 1.99 Å and to 2.16 Å, respectively. Consequently, the Bi–Bi interaction mediated by larger halogen ions is stronger with larger orbital overlap, leading to larger hopping and more dispersive bands. This in turn leads to smaller SOC-induced energy gap for Bi@Br-Si(111) (0.6 eV) and Bi@I-Si(111) (0.4 eV) (Fig. S2C and D). In general, the Bi–Bi interaction can also be tuned by choosing different semiconductor substrates, which is an interesting topic for future study.

Electronic and Topological Properties of Freestanding Planar Bi/Au Hexagonal Lattice

Fig. S3A and B show the calculated band structures and density of states (DOS) around Fermi level of Bi and Au, respectively. The planar Bi lattice has $Z_2 = 0$, and the Au lattice has $Z_2 = 1$. More generally, we can better understand the topological phases in a 2D hexagonal lattice by a multiorbital tight-binding model. The effective Hamiltonian with the nearest-neighbor hopping and intrinsic SOC can be written as:

$$\hat{H} = \sum_{i,l} \varepsilon_l c_{il}^\dagger c_{il} - \sum_{\langle i,j \rangle, l, l'} (t_{ijll'} c_{il}^\dagger c_{jl'} + H.c.) + \lambda_{SO} \hat{L} \cdot \hat{\sigma}, \quad [\text{S1}]$$

where c_{il}^\dagger creates an electron of l th orbital ($s, p_x, p_y, p_z, d_{xy}, \dots$) at site i . ε_l ($t_{ijll'}$) denotes the on-site energy (hopping energy) and λ_{SO} is the strength of SOC. As mentioned above, the Bi lattice can be described by the p -orbital six-band model, as illustrated in Fig. S3C. Due to the planar symmetry, p_x and p_y orbitals hybridize to be distinguished from the p_z orbital, resulting in two branches of energy bands. The p_z branch of π and π^* bands is exactly the same as graphene (9). The (p_x, p_y) branch has four bands: two flat bands (p_f, p_f^*) bracketing two dispersive bands (p_d, p_d^*), which form a Dirac point at K point. The SOC opens a gap in the dispersive bands at K point and mixes the p_d and p_d^* bands into two sets of $p_d \pm i p_d^*$ bands encoding a nontrivial topology. Again, the two branches of bands are both topologically nontrivial, but their sum becomes trivial. The planar Au lattice can be described by the s -orbital two-band model, as illustrated in Fig. S3D. Without SOC, the two s orbitals hybridize into linearly dispersive twofold degenerate σ and σ^* bands, which touches at K point (Dirac point); the SOC opens a gap and mixes the σ and σ^* bands into two sets of $\sigma \pm i \sigma^*$ bands encoding a nontrivial topology.

There are two ways to make the planar hexagonal Bi lattice topologically nontrivial. The first way is by the well-known band-inversion approach (10), which in the present case can be achieved by buckling the lattice into a nonplanar structure (Fig. S4A), i.e., the single Bi(111) bilayer. Fig. S4B shows the band structure and DOS of a Bi(111) bilayer, which is confirmed with nontrivial topology (11). In such a buckled structure, the Bi–Bi bond angle is around 90°, indicating that three (p_x, p_y , and p_z) orbitals are degenerate with each other. Chemical bonding and crystal field splitting lifts the degeneracy and form one set of doubly degenerate $\sigma_{1,2}$ and $\sigma_{1,2}^*$ bands and another set of non-degenerate σ_3 and σ_3^* bands, in the order of energy as shown in Fig. S4C. The SOC opens an energy gap and further lifts the degeneracy of $\sigma_{1,2}$ and $\sigma_{1,2}^*$ bands, as well as causes a band inversion of energy order between $\sigma_{1 \pm i 2}$ and σ_3^* bands around the Fermi level. Consequently, the overall band topology becomes nontrivial.

The second approach is to simply remove one branch of orbitals [either (p_x, p_y) or p_z] to reduce the trivial six-band lattice into a nontrivial two- or four-band lattice. To verify this idea, we artificially saturate the planar hexagonal Bi lattice with H to remove the p_z orbital (Fig. S4D). It is found that the p_z orbital of Bi hybridizes strongly with s orbital of H, shifting away from the Fermi level, so that the system reduces to a (p_x, p_y)-orbital four-band model, which supports a nontrivial topological phase (Fig. S4E and F). This is essentially what happens with the Bi@Cl-Si(111), where the exposed Si atom in the Cl-Si(111) surface fulfills the role of H atom to remove the p_z orbital of Bi.

- Blöchl PE (1994) Projector augmented-wave method. *Phys Rev B Condens Matter* 50(24):17953–17979.
- Kresse G, Joubert D (1999) From ultrasoft pseudopotentials to the projector augmented-wave method. *Phys Rev B* 59:1758.
- Kresse G, Hafner J (1993) *Ab initio* molecular dynamics for liquid metals. *Phys Rev B Condens Matter* 47(1):558–561.
- Perdew JP, Burke K, Ernzerhof M (1996) Generalized gradient approximation made simple. *Phys Rev Lett* 77(18):3865–3868.
- Heyd J, Scuseria GE, Ernzerhof M (2006) Hybrid functionals based on a screened Coulomb potential. *J Chem Phys* 124:219906.
- Henkelman G, Uberuaga BP, Jónsson H (2000) A climbing image nudged elastic band method for finding saddle points and minimum energy paths. *J Chem Phys* 113:9901.
- Singh DJ, Nordstrom L (1994) *Planewaves, Pseudopotentials and the LAPW Method* (Kluwer Academic, Boston).
- Fukui T, Hatsugai Y (2007) Quantum spin Hall effect in three dimensional materials: Lattice computation of Z_2 topological invariants and its application to Bi and Sb. *J Phys Soc Jpn* 76:053702.
- Kane CL, Mele EJ (2005) Quantum spin Hall effect in graphene. *Phys Rev Lett* 95(22):226801.
- Bernevig BA, Hughes TL, Zhang SC (2006) Quantum spin Hall effect and topological phase transition in HgTe quantum wells. *Science* 314(5806):1757–1761.
- Liu Z, et al. (2011) Stable nontrivial Z_2 topology in ultrathin Bi (111) films: A first-principles study. *Phys Rev Lett* 107(13):136805.

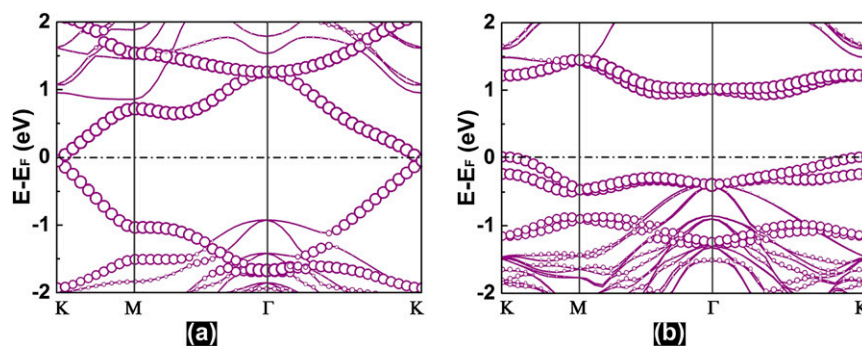


Fig. S1. Band structures for Bi@Cl-Si(111) surface system calculated by using hybrid function of ref. 5. (A) Without and (B) with SOC. Bands compositions are indicated, with size of circles denoting the contribution from Bi.

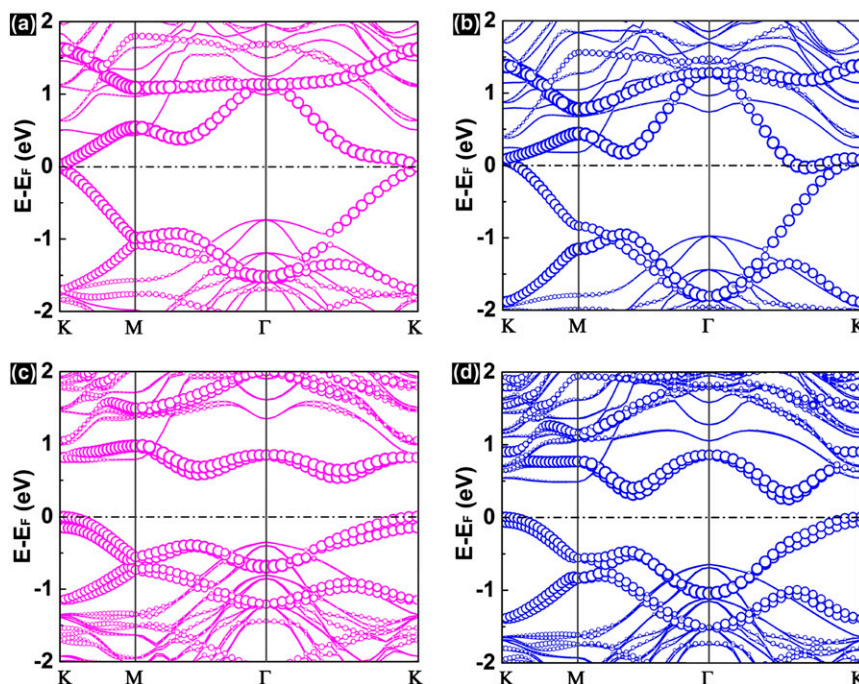


Fig. S2. Band structures for Bi@Br (l)-Si(111). (A and B) Band structures for Bi@Br-Si(111) and Bi@I-Si(111) surface structure without SOC, respectively. (C and D) As in A and B, but with SOC. Bands compositions are indicated as in Fig. S1.

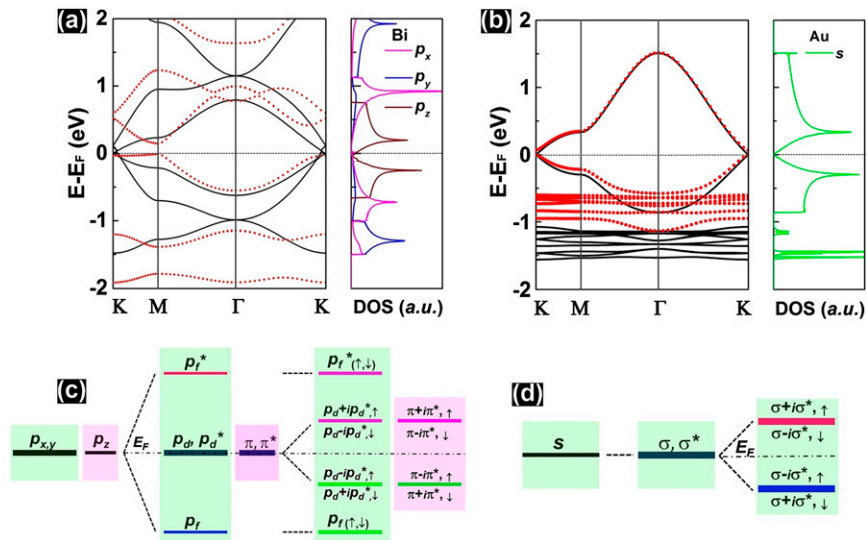


Fig. S3. Band structure, DOS, and energy diagram of planar Bi and Au hexagonal lattice. (A) Band structure without (black solid curves) and with SOC (red dotted curves) of a planar hexagonal lattice of Bi, along with the atomic-orbital-projected DOS without SOC. (B) As in A, but for Au. (C and D) The energy diagrams of the Bi and Au lattices at K point illustrating the effects of orbital hybridization and SOC.

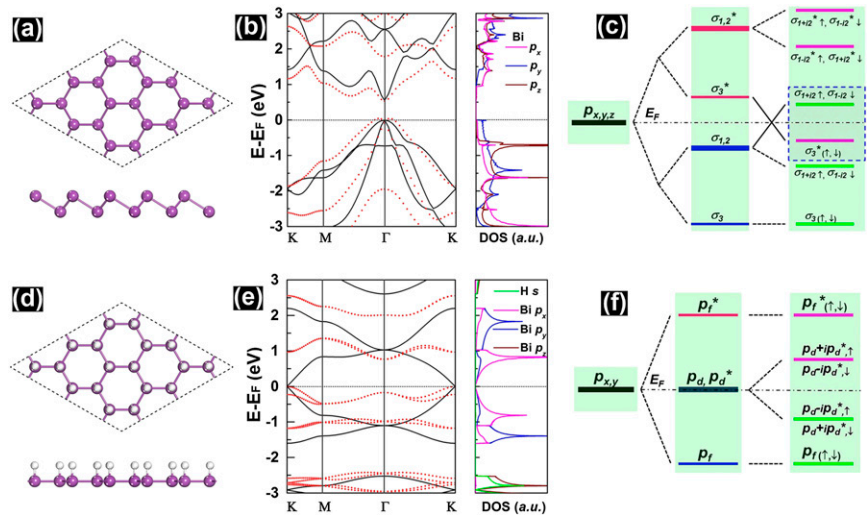


Fig. S4. Band structure, DOS, and energy diagram of buckled and H-saturated Bi hexagonal lattice. (A–C) Structural model, band structure, and atomic-orbital-projected DOS, and the energy diagram (at Γ point), respectively, of a buckled Bi(111) bilayer. The band inversion is highlighted by a dashed rectangle. (D–F) As in A–C, but for planar Bi hexagonal lattice with one side saturated by H.